symmetry

MDPI

Article

Nuclear Spin-Dependent Effects of Parity Nonconservation in Ortho-H_2

Dmitry V. Chubukov [1,2,*], Leonid V. Skripnikov [1,2], Leonti N. Labzowsky [1,2] and Günter Plunien [3]

1 Department of Physics, St. Petersburg State University, 7/9 Universitetskaya Naberezhnaya, 199034 Saint Petersburg, Russia; leonidos239@gmail.com (L.V.S.); l.labzovskii@spbu.ru (L.N.L.)
2 Petersburg Nuclear Physics Institute Named by B.P. Konstantinov of National Research Centre "Kurchatov Institut", St. Petersburg, 188300 Gatchina, Russia
3 Institut für Theoretische Physik, Technische Universität Dresden, D-01062 Dresden, Germany; Guenter.Plunien@tu-dresden.de
* Correspondence: dmitrybeat@gmail.com

Received: 27 November 2019; Accepted: 8 January 2020; Published: 10 January 2020

Abstract: We report a theoretical treatment of the nuclear spin-dependent spatial parity nonconserving (NSD-PNC) electron–nuclear interaction effect in the diatomic homonuclear ortho-H_2 molecule. The magnetic dipole transition between $v = 1$ and $v = 0$ vibrational sublevels of the ground $^1\Sigma_g^+$ state is examined. The orthohydrogen molecule is a unique molecular system where the parity nonconserving (PNC) nuclear spin-dependent interaction due to the neutral weak currents can be directly observed and the corresponding coupling constant can be extracted from the future experiments. The theoretical simulation shows that using the cavity-enhanced scheme in conjunction with the record achievement of the intracavity absorption spectroscopy, the experiment on the observation of the NSD-PNC effect due to the neutral weak current in ortho-H_2 looks feasible.

Keywords: parity nonconservation; orthohydrogen molecule; weak neutral currents

1. Introduction

Investigation of spatial parity ($\mathcal{P}$) violation effects at low energies is an effective tool for developing models of fundamental interactions in physics. Hypothesizing of the neutral weak current led to development of the standard model (SM) [1–3]. The claim of the SM stimulated to search for the $\mathcal{P}$-odd effects in different atomic and molecular systems. However, to extract the SM parameters from the atomic (or molecular) experiments, one needs to perform considerably sophisticated theoretical calculations, since all electrons contribute to such effects. There are two main types of experiments to search for the spatial parity nonconserving (PNC) interactions in atomic (or molecular) systems. The first type is the optical dichroism observation, i.e., the observation of asymmetry in the number of emitted (absorbed) left- or right-handed photons. Such experiments were proposed by M. Bouchiat and C. Bouchiat on Cs [4] and performed by the Wieman group later [5]. This is the most accurate experiment in a low-energy regime that supports the SM theory and strongly restricts any "new physics" beyond it (see, e.g., the review [6]). The second type of experiments is the optical rotation of the light polarization plane in atomic (molecular) vapors. It was originally proposed by Khriplovich on Bi [7] and performed by Barkov and Zolotorev [8].

Systems with a simpler electronic structure are of interest due to a more direct theoretical interpretation. In neutral atoms, the $\mathcal{P}$-odd electron–nuclear (e–N) interaction effect increases approximately as Z^3 with the charge of the nucleus Z [4,9]. Therefore, a reasonable choice could be few-electron heavy highly charged ions (HCI). They have large nuclear charges and it is possible

to perform very accurate calculations of their electronic structure. In [10], it was proposed for the first time to observe the PNC effects in He-like HCI. Such proposal was stimulated by the crossing of opposite parity levels with certain Z values. Despite a number of suggestions to search for the PNC effects in HCI, no experimental results have been reported. Recently, a new PNC experiment with HCI in storage rings has been proposed in [11] where it was suggested to employ a new method of preparation of polarized HCI nuclei—by the polarized electrons capture.

In most of atomic experiments to study PNC effects, the $\mathcal{P}$-odd electron–electron (e–e) interaction is hidden by the $\mathcal{P}$-odd e–N one. The latter usually dominates [4,9,12,13]. The $\mathcal{P}$-odd e–e interaction was observed exclusively at high energies by the SLAC collaboration [14]. Up to now, there were no other evidence for the presence of the PNC e–e interaction. In [15], it was proposed to measure PNC optical rotation due to the weak e–e interaction on the oxygen molecule which assumed to be the dominant source of the parity violation due to the formation of a chemical bond. Recent calculation of the PNC effects in the O_2 molecule [16] showed that the enhancement of the PNC e–e exists in this case, compared to the atomic one, but still, the effect is suppressed compared to the dominant PNC e–N interaction. In [17], it was shown that the favorable situation for observation of the PNC e–e interaction effect appears in the para-H_2 molecule.

In an atomic experiment, [5], on the nuclear spin-dependent (NSD) parity violating the e–N interaction effect observation, the value of the nuclear anapole moment was extracted. The effect of the electromagnetic interaction of electrons with the anapole moment of the nucleus prevails over other sources of the PNC-NSD e–N interaction effects in heavy atomic systems. In that way, nuclear spin-dependent spatial parity nonconserving (NSD-PNC) effects due to the nuclear anapole moment were also observed by the Wieman group [5]. However, the hydrogen molecule is the unique molecular system in which the dominant source of the NSD parity violation is due to the neutral weak current interaction. Therefore, it is the favorable system to extract the coupling constant for this interaction, the Weinberg angle, in order to test the SM and put constraints on its extensions.

The aim of this paper is to complete the investigation of PNC effects in the H_2 molecule and to perform ab-initio calculations of the nuclear spin-dependent part of the PNC effects in orthohydrogen. In the ortho-H_2 molecule, the total nuclear spin is equal to one. The magnetic dipole (M1) transition between different vibrational sublevels with the same rotational numbers of the ground electronic state $X^1\Sigma_g^+$ of the orthohydrogen molecule is considered. In [18] it was demonstrated that such transitions in the H_2 molecule are of the M1 type. The M1 amplitude is nonzero due to the nonadiabatic corrections. Note that for the observation of the parity violating effects it is favorable to use the M1 transitions [9]. Here we also demonstrate that using the cavity-enhanced scheme (reported in [19]) and record achievement of the intracavity absorption spectroscopy (ICAS) (described in [20,21]) the experiment on the observation of the PNC-NSD effect due to the neutral weak current in the orthohydrogen molecule looks feasible enough.

2. Theory

Here we study the parity violation mechanism in the transition between $v_1 = 1$ and $v_0 = 0$ vibrational sublevels of the ground electronic state $^1\Sigma_g^+$ of the orthohydrogen molecule. The initial and the final states have equal rotational numbers $N = J$, where $\mathbf{N}$ is the total angular momentum of the molecule less the electron spin.

Owing to the spatial symmetry violation produced by an effective operator of PNC interaction $V_{\mathcal{P}}$ the gerade (g) wave function of the H_2 ground state gets the admixture of the whole spectrum of the ungerade (u) ones (i.e., of the opposite parity). As a consequence of such mixing, the pseudoscalar term appears in the probability of the considered process:

$$W = W^{\mathrm{M1}}(1 + (\boldsymbol{s}_{ph} \cdot \boldsymbol{\nu})\mathcal{P}). \quad (1)$$

Here we introduced the factor $\mathcal{P}$—the PNC, or the circular polarization degree. In our case the pseudoscalar term is $(\boldsymbol{s}_{ph} \cdot \boldsymbol{\nu})$, where $\boldsymbol{s}_{ph} = i(\boldsymbol{e} \times \boldsymbol{e}^*)$ is the spin of photon, $\boldsymbol{\nu}$ is the direction of photon emission, $\boldsymbol{e}$ is the polarization of photon. In a general way

$$i\mathcal{P} = 2\frac{\mathrm{E1}^{\mathrm{PNC}}_{gv_1 \to gv_0}}{\mathrm{M1}_{gv_1 \to gv_0}}, \tag{2}$$

where $\mathrm{E1}^{\mathrm{PNC}}_{gv_1 \to gv_0}$, $\mathrm{M1}_{gv_1 \to gv_0}$ are the PNC-induced electric dipole and the ordinary magnetic dipole amplitudes between the states of the same parity (g), respectively.

$$\begin{aligned} \mathrm{E1}^{\mathrm{PNC}}_{f,gv_1 \to gv_0} &= \sum_{i,j,k} \left(\frac{\langle gv_1 J|(\boldsymbol{d})_f|u_i v_j N_k J\rangle \langle u_i v_j N_k J|V_{eN}|gv_0 J\rangle}{E_{gv_0 J} - E_{u_i v_j N_k}} \right. \\ &+ \left. \frac{\langle gv_1 J|V_{eN}|u_i v_j N_k J\rangle \langle u_i v_j N_k J|(\boldsymbol{d})_f|gv_0 J\rangle}{E_{gv_1 J} - E_{u_i v_j N_k}} \right), \end{aligned} \tag{3}$$

$$\mathrm{M1}_{q,gv_1 \to gv_0} = \langle gv_1 J|(\boldsymbol{\mu})_q|gv_0 J\rangle. \tag{4}$$

In Equation (3) the electric dipole operator $\boldsymbol{d}$ and in Equation (4) the magnetic dipole operator are introduced. A spherical components of $\boldsymbol{d}$ and $\boldsymbol{\mu}$ are denoted by the letters f and q, respectively. Since the considered interaction is the $\mathcal{T}$-invariant one, the PNC matrix element is imaginary [9].

Within the SM framework, the effective operator describing NSD parity violating e–N interaction for the case of the diatomic molecule is given by

$$V_{eN} = \frac{G_F}{\sqrt{2}} \frac{\kappa}{I} \boldsymbol{\alpha} \boldsymbol{I} \left(\rho(\boldsymbol{r}) + \rho(\boldsymbol{r} - \boldsymbol{R}) \right), \tag{5}$$

where $G_F = 1.027 \times 10^{-5} \hbar c \left(\frac{\hbar}{m_p c} \right)^2 = 2.22249 \times 10^{-14}$ a.u. is the Fermi constant (m_p is the proton mass), $\boldsymbol{I}$ is the nuclear spin, $\boldsymbol{\alpha}$ is the Dirac matrix, $\rho(\boldsymbol{r})$ is the normalized to 1 nuclear density distribution and R is the internuclear distance. From Equation (5) it follows that the effect of the NSD-PNC e–N interaction is proportional to the dimensionless constant κ. It includes three major types of contributions (see the review [6]). The first one arises from electromagnetic interaction of electrons with the anapole moment of the nucleus [22,23]. In a simple nuclear shell model [23] for heavy nuclei this contribution κ_A can be estimated as

$$\kappa_A \approx 1.15 \times 10^{-3} \frac{K}{I+1} A^{2/3} \mu_N g_N, \tag{6}$$

where $K = (-1)^{I+1/2-l} (I + 1/2)$ (l is the orbital angular momentum of the single unpaired nucleon), μ_N and g_N are the magnetic moment in nuclear magnetons and the weak coupling constant of the unpaired nucleon, A is the number of nucleons. The next contribution arises from the electron–nucleus NSD neutral weak-current interaction [24]. In the nuclear shell model this contribution κ_2 reads

$$\kappa_2 = \frac{1/2 - K}{I+1} C_2, \tag{7}$$

where C_2 is the coupling constant for the valence nucleon. For protons and neutrons it can be expressed as follows:

$$C_{2p} = -C_{2n} = -\frac{\lambda}{2} \left(1 - 4 \sin^2 \theta_W \right). \tag{8}$$

Here $\lambda = 1.25$, θ_W is the Weinberg angle. In our paper, we approximate the Weinberg angle as $\sin^2 \theta_W \approx 0.23$. The last contribution arises from the effect of the nuclear spin-independent $e - N$

interaction combined with the magnetic hyperfine interaction [25] (i.e., appears as the radiative correction to NSI-PNC effect). This contribution κ_Q can be estimated as (see, e.g., [6])

$$\kappa_Q \approx 2.5 \times 10^{-4} A^{2/3} \mu_N. \tag{9}$$

The κ constant thus reads

$$\kappa = \kappa_A + \kappa_2 + \kappa_Q. \tag{10}$$

In heavy atomic and molecular systems usually the anapole moment contribution dominates, i.e., from all previous experiments on the search for the NSD-PNC interaction effects the anapole moment of the nucleus was usually extracted. Let us estimate the contributions to κ for the case of the orthohydrogen molecule. In our case Equation (6) is not valid, since the nuclei are pure protons. In [26] it was shown that each particle with nonzero spin possesses an intrinsic anapole moment due to radiative corrections to the PNC-NSD e–N interaction and thus can be attributed to the κ_2 constant. In [9] an upper bound of this contribution was roughly estimated as $\kappa_A = \kappa_{2,\mathrm{rad.corr}} \sim 10^{-3}$. In the present case Equation (9) also yields in upper bound for the value of κ_Q. Since we have unpaired protons in the system considered, we use the value of $\mu_p = 2.8$. For one nucleus

$$\begin{aligned} \kappa_A &= \kappa_{2,\mathrm{rad.corr}} \lesssim 10^{-3}, \\ \kappa_2 &\approx -0.05, \\ \kappa_Q &\lesssim 7.0 \times 10^{-4}. \end{aligned} \tag{11}$$

From Equation (11) it follows that the orthohydrogen molecule is the unique molecular system where the dominant source of parity violating NSD effects is the e-N neutral weak-current interaction and where the C_2 coupling constant can be directly observed.

The ground electronic state $^1\Sigma_g^+(0_g^+)$ of the orthohydrogen contains only odd rotational numbers $N = J$ [27]. The NSD-PNC operator (Equation (5)) is an electronic vector, so the matrix of this operator can contain $|\Delta\Omega| = 0, 1$ entries. However, the major contribution to the effect considered is arising from the mixing of $^1\Sigma_g^+(0_g^+)$ ground state and $^1\Pi_u$ states (since the admixed E1 $^1\Pi_u \to {}^1\Sigma_g^+$ transition is allowed). Besides, $^1\Pi_u^\pm = \frac{1}{\sqrt{2}}\left(|\Lambda = 1\rangle \pm (-1)^{N+\Lambda}\,|\Lambda = -1\rangle\right)$. In homonuclear orthohydrogen molecule for each rotational quantum number N only the $^1\Pi_u^+$ state survives.

Spatial parity violation interaction leads to the interference between M1 and PNC-induced E1 amplitudes. The derivation of explicit expressions for them is based on the use of complete wave function of the molecule that takes into account also nuclear spin variables. Applying the Wigner–Eckart theorem and using the expression for the matrix element of a single operator in a coupled scheme (see, e.g., [28]), we express the M1 amplitude via the reduced matrix element:

$$\begin{aligned} \mathrm{M1}_{q,gv_1\to gv_0} &= \langle FM_F JIv_1(^1\Sigma_g^+)|(\boldsymbol{\mu})_q|FM_F' JIv_0(^1\Sigma_g^+)\rangle \\ &= (-1)^{2F+I+J+1-M_F}(2F+1)\cdot \begin{pmatrix} F & 1 & F \\ -M_F & q & M_F' \end{pmatrix} \begin{Bmatrix} J & F & I \\ F & J & 1 \end{Bmatrix} \cdot \langle gJv_1||\mu||gJv_0\rangle. \end{aligned} \tag{12}$$

Here $\langle gJv_1||\mu||gJv_0\rangle = \sqrt{J(J+1)(2J+1)}\mu_N\langle v_1|g(R)|v_0\rangle$, where the nuclear magneton μ_N and the rotational g-factor g was introduced. Note that the vibrational wave-functions that correspond to different vibrational sublevels of the same electronic level are orthogonal to each other ($\langle v_1|v_0\rangle = 0$). However, in [18], it was shown that this g-factor depends on R due to the nonadiabatic corrections, therefore such M1 amplitudes are different from zero. In what follows the M1 amplitudes from [18] are employed. According to [18], $\mu_N\langle v_1|g(R)|v_0\rangle \approx (4-5)\times 10^{-8}\, ea_0$ for $J = (2-30)$ (e is the charge of the electron and a_0 is the Bohr radius), i.e., they weakly depends on J.

Now let us write $\mathrm{E1}^{\mathrm{PNC}}$ transition amplitudes with intermediate admixed $^1\Pi_u^+$ terms. For simplicity we consider only $|\Lambda = 1\rangle$ term in $^1\Pi_u^+$. Similar derivations show that the contribution of $|\Lambda = -1\rangle$ term is equal to the $|\Lambda = 1\rangle$ one. Performing angular reduction gives the following result:

$$\sum_{M_F''ijk} \langle gv_1 FM_F JI(^1\Sigma_g^+)|(\boldsymbol{d})_f|u_i v_j N_k FM_F'' J' I(\Lambda = 1)\rangle\langle u_i v_j N_k FM_F'' J' I(\Lambda = 1)|\boldsymbol{\alpha I}|gv_0 FM_F' JI(^1\Sigma_g^+)\rangle$$

$$= \sum_{M_F''ijk} (-1)^{2F+J+I+1-M_F}(2F+1)\begin{pmatrix} F & 1 & F \\ -M_F & f & M_F'' \end{pmatrix}\begin{Bmatrix} J' & F & I \\ F & J & 1 \end{Bmatrix}\langle gv_1 J||\boldsymbol{d}||u_i v_j N_k J(\Lambda = 1)\rangle$$

$$\times(-1)^{F+J+I}\begin{Bmatrix} I & J & F \\ J' & I & 1 \end{Bmatrix}\delta_{M_F' M_F''}\langle u_i v_j N_k J'(\Lambda = 1)||\boldsymbol{\alpha}||gv_0 J\rangle\sqrt{I(I+1)(2I+1)}. \quad (13)$$

Performing now the transformation from the laboratory frame of reference to the molecule-fixed frame according to [27,28] results in

$$\sum_{M_F''ijk} \langle gv_1 FM_F JI(^1\Sigma_g^+)|(\boldsymbol{d})_f|u_i v_j N_k FM_F'' J' I(\Lambda = 1)\rangle\langle u_i v_j N_k FM_F'' J' I(\Lambda = 1)|\boldsymbol{\alpha I}|gv_0 FM_F' JI(^1\Sigma_g^+)\rangle$$

$$= \sum_{ijJ'}(-1)^{3F+2J+2I+1-M_F}(2F+1)\,s(J')\sqrt{I(I+1)(2I+1)}\begin{pmatrix} F & 1 & F \\ -M_F & f & M_F' \end{pmatrix}$$

$$\times\begin{Bmatrix} J' & F & I \\ F & J & 1 \end{Bmatrix}\langle gv_1|d_-|u_i v_j(\Lambda = 1)\rangle\begin{Bmatrix} I & J & F \\ J' & I & 1 \end{Bmatrix}\langle u_i v_j'(\Lambda = 1)|\alpha_+|gv_0\rangle. \quad (14)$$

Here $s(J') = s(N_k)$ (since we consider only singlet molecular states) is the constant that arises from the transformation to the molecule-fixed frame. Note that $s(J' = J) = (2J+1)/4$, $s(J' = J+1) = (J+2)/4$ and $s(J' = J-1) = (J-1)/4$ [27].

Denoting

$$S = \sum_{J'}(-1)^{3F+2J+2I+1}(2F+1)\,s(J')\sqrt{I(I+1)(2I+1)}\begin{Bmatrix} J' & F & I \\ F & J & 1 \end{Bmatrix}\begin{Bmatrix} I & J & F \\ J' & I & 1 \end{Bmatrix} \quad (15)$$

and summing over the M_F' projections in the M1 and E1 interference contribution it follows that

$$\mathrm{E1}^{\mathrm{PNC}}_{gv_1 \to gv_0} = S\frac{2\kappa}{I}\sum_{i,j}\left(\frac{\langle gv_1|d(R)|u_i v_j\rangle\langle u_i v_j|W_{eN}(R)|gv_0\rangle}{E_{gv_0} - E_{u_i v_j}} - \frac{\langle gv_1|W_{eN}(R)|u_i v_j\rangle\langle u_i v_j|d(R)|gv_0\rangle}{E_{gv_1} - E_{u_i v_j}}\right). \quad (16)$$

In Equation (16)

$$\begin{aligned} d(R) &= \langle g(0_g^+)|d_-|^1\Pi_u(\Lambda = 1)\rangle, \\ W_{eN}(R) &= \langle ^1\Pi_u(\Lambda = 1)|\frac{G_F}{\sqrt{2}}\rho(\boldsymbol{r})\alpha_+|g(0_g^+)\rangle. \end{aligned} \quad (17)$$

The minus sign in Formula (16) is due to the imaginary matrix element $W_{eN}(R)$. The choice of the hyperfine sublevel depends on the certain experimental conditions. For different F and J, the coefficient S ranges between ~ 0.1 and ~ 2. Without restricting the generality we set $S = 1$. The same holds true for the coefficient at the reduced matrix element of μ for M1 amplitude in Equation (12).

3. Electronic Structure Calculation Details

Calculations of electronic structure of the hydrogen molecule have been performed within the configuration interaction with single and double excitations method using the Dirac–Coulomb Hamiltonian. For H atoms the dyall.aae4z basis set has been used from the directory of the

DIRAC15 [29] code. The latter has been used to perform Dirac–Hartree–Fock calculations and integral transformation. Configuration interaction calculations have been performed within the MRCC code [30,31]. Matrix elements of the parity nonconserving electron–nucleus interaction operator were calculated within the code developed in this paper.

Electronic energies and matrix elements $W_{eN}(R)$, $d(R)$ have been calculated for twenty values of the internuclear distance R for the hydrogen molecule. Using the obtained potential energy curves for the ground and the excited $C^1\Pi_u^+$ states, the vibrational wave functions for these states have been calculated within the VIBROT code [32]. This code has also been used to calculate values of d and W_{eN} characteristics averaged over these vibrational wave functions as well as the spectroscopic parameters of considered molecular terms. Values of these parameters are given in Table 1. One can see a good agreement between the theoretical and experimental values. Theoretical uncertainty of the calculations can be estimated as 10%.

Table 1. Comparison of the results obtained in the present paper for the $X^1\Sigma_g^+$ and $C^1\Pi_u$ internuclear equilibrium distances, spectroscopic constants B_e, and also the electronic energy of the excited $C^1\Pi_u$ state with corresponding experimental data from [33]. r_0 is the equilibrium internuclear distance in units of the Bohr radius a_0 and T_e is the minimum electronic energy in cm^{-1}.

	Present Paper $X^1\Sigma_g^+$	**Experiment [33]** $X^1\Sigma_g^+$	**Present Paper** $C^1\Pi_u$	**Experiment [33]** $C^1\Pi_u$
r_0 (a_0)	1.407	1.401	1.94	1.952
T_e (cm^{-1})	-	-	103309	100090
B_e (cm^{-1})	58.4	60.853	30.6	31.362

4. Results and Discussion

In the present work we took into account the contribution originating from the mixing between the ground and the first excited $C^1\Pi_u^+$ state. Note also that the energy denominators in Equation (3) for higher excited terms are larger, thus within the claimed uncertainty (about 10%) their total contribution to the parity violating effects can be neglected. The calculated dependencies of the imaginary component of W_{eN} and the E1 matrix element on R are given in Figure 1a,b.

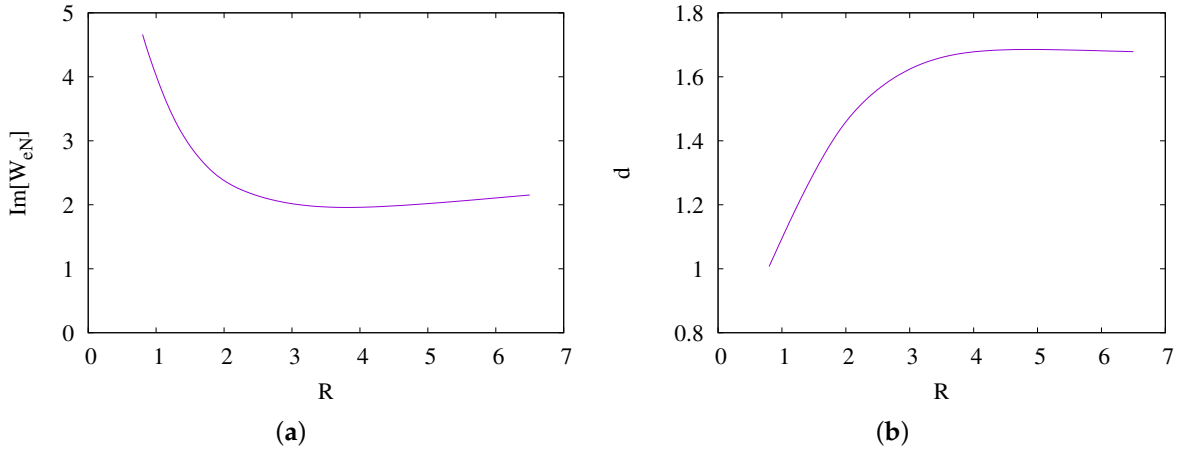

Figure 1. In (**a**) the dependence of the imaginary component Im[W_{eN}] of the nuclear spin-dependent spatial parity nonconserving (NSD-PNC) e–N matrix element in the units of 10^{-2} Hz is represented as function of the internuclear distance R in the units of the Bohr radius a_0 (see Equation (17)); (**b**) depicts the dependence of the transition dipole moment matrix element in ea_0 (e is the electron charge) on the internuclear distance R in the units of the Bohr radius (see Equation (17)). Both (**a**) and (**b**) correspond to the case of mixing between $C^1\Pi_u$ and $X^1\Sigma_g^+$.

The final result for the nuclear spin-dependent $E1^{PNC}$ amplitudes in ortho-H_2 is as follows:

$$E1_{eN}^{PNC} = 3.8 \times 10^{-7} G_F[\text{a.u.}]\ iea_0. \tag{18}$$

Then, the parity nonconserving degree for the effect considered now reads

$$\mathcal{P}_{eN} = \frac{1}{\sqrt{J(J+1)(2J+1)}} 4.2 \times 10^{-13}. \tag{19}$$

Note that according to [17] the nuclear spin-independent PNC effects for the molecular system considered are negligible compared to the NSD-PNC one.

Finally, we perform an analytical modeling of the PNC optical rotation experiment on the ortho-H_2 molecule. In what follows we will use the record achievements of the cavity-enhanced polarimetric scheme introduced in [19] and intracavity absorption spectroscopy (ICAS) discussed in [20,21]: the record optical pathlength 7×10^4 km and the record shot-noise-limited birefringence-phase-shift sensitivity 3×10^{-13} rad. In our derivations, one should take into account the light absorption while propagating through the medium. Obviously, working at the resonance frequency of the considered transition, the laser light will be immediately absorbed. But in [19], the possibility to shift off-resonance in such ICAS experiment is discussed. For the off-resonance measurements the PNC optical rotation angle reaches its maximum value and the absorption is too small (see, e.g., [9]). The rotation angle in optical experiments increases with the optical pathlength l linearly. The light transmission through a medium is governed by the Beer–Lambert law [34], that is, falls as e^{-l/l_0} (l_0 is the absorption length). The PNC signal (the product of the rotation angle and the light transmission) $\sim l e^{-l/l_0}$. So the optimal signal-to-noise ratio corresponds to $l = 2l_0$ [9,35].

The PNC optical rotation angle φ_{PNC} can be expressed as [9]

$$\varphi_{\text{PNC}} = -\frac{4\pi l}{3\hbar c} \frac{\omega}{\Gamma_D} \frac{\rho}{2F+1} g(u,v) \langle gJv_1||\mu||gJv_0\rangle \text{Im}[E1_{eN}^{PNC}]. \tag{20}$$

Here ρ is the vapor number density and ω resonance frequency of the transition, Γ_D is the Doppler width. The latter can be expressed as [9]

$$\Gamma_D = \omega\beta(T), \tag{21}$$

where $\beta(T) = \sqrt{\frac{2k_BT}{Mc^2}}$. Here M is the molecule mass, T is the absolute temperature and k_B is the Boltzmann constant. The Voigt profile can be introduced as:

$$\mathcal{F}(u,v) = \sqrt{\pi} e^{-(u+iv)^2} \left[1 - \text{Erf}(-i(u+iv))\right]. \tag{22}$$

Here we introduced two dimensionless variables. u is determined in the following way:

$$u = \frac{\Delta\omega}{\Gamma_D}, \tag{23}$$

where $\Delta\omega$ is the detuning of the frequency. Variable v is determined by

$$v = \frac{\Gamma}{\Gamma_D}, \tag{24}$$

where Γ is the collisional broadening width (in the case of forbidden M1 transition the contribution originating from the natural line width is negligible) and

$$\Gamma \sim \rho\sigma_{\text{col}}\beta(T)c, \tag{25}$$

where $\sigma_{\rm col}$ is the collisional cross-section. The $g(u,v)$ function in Equation (20) can be expressed via the Voigt profile in the following way:

$$g(u,v) \equiv \mathrm{Im}\ \mathcal{F}(u,v). \tag{26}$$

The quantity inverse to the absorption length reads

$$l_0^{-1} = \frac{4\pi}{3\hbar c}\frac{\omega}{\Gamma_D}\frac{\rho}{2F+1} f(u,v)\langle gJv_1||\mu||gJv_0\rangle^2, \tag{27}$$

where

$$f(u,v) \equiv \mathrm{Re}\ \mathcal{F}(u,v). \tag{28}$$

For $u \gg 1$ (i.e., for the off-resonance measurements) the $g(u,v)$ and $f(u,v)$ functions have the following asymptotics:

$$\begin{aligned} g(u,v) &\approx \frac{1}{u}, \\ f(u,v) &\approx \frac{v}{u^2}. \end{aligned} \tag{29}$$

Using the condition $l = 2l_0$ [9,35] of the optimal signal-to-noise relation, as well as Equations (20)–(29), one obtains

$$\rho = \sqrt{\frac{3(2F+1)\hbar\beta(T)\omega u^2}{2\pi l \mu_N^2 \langle v_1|g(R)|v_0\rangle^2 J(J+1)(2J+1)\sigma_{\rm col}}}, \tag{30}$$

$$\varphi_{\rm PNC} = 3.8\times 10^{-7}\,(G_F[\text{a.u.}])\sqrt{\frac{8\pi l\omega}{3\hbar c^2\beta(T)\sigma_{\rm col}(2F+1)}}\,ea_0. \tag{31}$$

Equation (27) is valid only for $J > 20$ when the electric quadrupole amplitude is less than the magnetic dipole one (see [18]). Note that for $J < 20$ there is an additional absorption originating from the E2 contribution, thus the PNC effect is suppressed. In what follows we use $J \sim 25$. Since $\varphi_{\rm PNC} \sim \beta^{-1/2}(T) \sim T^{-1/4}$, cooling of molecular vapor does not improve the situation. We use $\omega \approx 8\times 10^{14}$ s^{-1}, the characteristic value of the collision cross section for H_2 $\sigma_{\rm col} \approx 10^{-15}$ cm^2, $T = 300$ K, $l = 7\times 10^4$ km [20]. Then the optimal PNC optical rotation angle can be estimated as

$$\varphi_{\rm PNC} \sim 3\times 10^{-13}\ \text{rad}. \tag{32}$$

The value of the PNC rotation angle in Equation (32) corresponds to the number density

$$\rho \sim 10^{17}\ \text{cm}^{-3}. \tag{33}$$

It is worth to mention again that using cavity-enhanced scheme the record shot-noise-limited birefringence phase-shift at the level 3×10^{-13} rad has been demonstrated [21].

5. Conclusions

In this paper we have calculated the expected effect caused by the nuclear spin dependent parity nonconserving interaction due to the neutral weak current in ortho-H_2. This molecule is the unique candidate to search for this effect as it will be the dominating one among other PNC effects (especially among the electromagnetic interaction of the anapole moment of the nucleus with the electrons). This is usually not the case for other atomic and molecular experiments to search for the PNC effects. Obtained prediction of the PNC rotation angle is of the same order as the record small angle measured by the cavity-enhanced technique [21].

Author Contributions: D.V.C., L.V.S., L.N.L., and G.P. are equally contributed. All authors have read and agreed to the published version of the manuscript.

Funding: The work of D.V.C. connected with the performance of all-electron calculation for the considered NSD-PNC electron–nucleus effect as well as preparing the paper was funded by RFBR according to the research project No. 18-32-00150. D.V.C. acknowledges also the support from the Foundation for the advancement of theoretical physics and mathematics "BASIS" grant according to the research project No. 17-15-577-1 and from the DAAD-Programm Ostpartnerschaften (TU Dresden). The work of L.V.S connected with the development of the code for computation of the matrix elements of the considered NSD-PNC electron–nucleus operator was supported by the President of Russian Federation Grant No. MK-2230.2018.2. L.V.S. acknowledges also the support from the Foundation for the advancement of theoretical physics and mathematics "BASIS" grant according to the research project No. 18-1-3-55-1.

Conflicts of Interest: The authors declare no conflict of interest.

References

1. Weinberg, S. Effects of a neutral intermediate boson in semileptonic processes. *Phys. Rev. D* **1972**, *5*, 1412. [CrossRef]
2. Salam, A. Weak and Electromagnetic Interactions. In Proceedings of the 8th Nobel Symposium, Lerum, Sweden, 19–25 May 1968; Wiley: New York, NY, USA, 1968.
3. Glashow, S.L. Partial-Symmetries of Weak Interactions. *Nuclear Phys.* **1961**, *22*, 579. [CrossRef]
4. Bouchiat, M.A.; Bouchiat, C.I. Parity violation induced by weak neutral currents in atomic physics. *J. Phys. (Paris)* **1974**, *35*, 899. [CrossRef]
5. Wood, C.S.; Bennett, S.C.; Cho, D.; Masterson, B.P.; Robertson, J.L.; Tanner, C.E.; Wieman, C.E. Measurement of parity nonconservation and an anapole moment in cesium. *Science* **1997**, *275*, 1759–1763. [CrossRef]
6. Ginges, J.S.; Flambaum, V.V. Violations of fundamental symmetries in atoms and tests of unification theories of elementary particles. *Phys. Rep.* **2004**, *397*, 63. [CrossRef]
7. Khriplovich, I.B. Possibility to Observe Parity Violation in Atomic Transitions. *Sov. Phys. JETP Lett.* ***1974***, 20, *315.*
8. Barkov, L.M.; Zolotorev, M.S. Observation of Nonconservation of Parity in Atomic Transitions. *Sov. Phys. JETP Lett.* **1978**, *27*, 357.
9. Khriplovich, I.B. *Parity Nonconservation in Atomic Phenomena*; Gordon and Breach: London, UK, 1991.
10. Gorshkov, V.G.; Labzowsky, L.N. Effects of parity nonconservation in heavy ions. *Sov. Phys. JETP Lett.* **1974**, *19*, 394.
11. Bondarevskaya, A.A.; Chubukov, D.V.; Mistonova, E.A.; Lyashchenko, K.N.; Andreev, O.Y.; Surzhykov, A.; Labzowsky, L.N.; Plunien, G.; Liesen, D.; Bosch, F.; et al. Considerations towards the possibility of the observation of parity nonconservation in highly charged ions in storage rings. *Phys. Scr.* **2018**, *93*, 025401. [CrossRef]
12. Gorshkov, V.G.; Klimchitskaya, G.L.; Labzovskii, L.N.; Melibaev, M. Electron-electron weak interaction in atoms and ions. *Sov. Phys. JETP* **1977**, *45*, 666.
13. Sushkov, O.P.; Flambaum, V.V. Parity nonconservation in heavy atoms due to weak electron-electron interaction. *Yad. Fiz.* **1978**, *27*, 1307.
14. Anthony, P.L.; Arnold, R.G.; Arroyo, C. SLAC-E158 collaboration. Precision Measurement of the Weak Mixing Angle in Møller Scattering. *Phys. Rev. Lett.* **2005**, *95*, 081601. [CrossRef] [PubMed]
15. Labzovsky, L.N. Effects of parity nonconservation in electronic spectra of molecules. *Sov. Phys. JETP* **1977**, *46*, 853.
16. Chubukov, D.V.; Skripnikov, L.V.; Andreev, O.Y.; Labzowsky, L.N.; Plunien, G. Effects of parity nonconservation in a molecule of oxygen. *J. Phys. B* **2017**, *50*, 105101. [CrossRef]
17. Chubukov, D.V.; Skripnikov, L.V.; Labzowsky, L.N.; Plunien, G. Nuclear spin-independent effects of parity nonconservation in molecule of hydrogen. *J. Phys. B* **2019**, *52*, 025003. [CrossRef]
18. Pachucki, K.; Komasa, J. Magnetic dipole transitions in the hydrogen molecule. *Phys. Rev. A* **2011**, *83*, 032501. [CrossRef]

19. Bougas, L.; Katsoprinakis, G.E.; von Klitzing, W.; Rakitzis, T.P. Fundamentals of cavity-enhanced polarimetry for parity-nonconserving optical rotation measurements: Application to Xe, Hg, and I. *Phys. Rev. A* **2014**, *89*, 052127. [CrossRef]
20. Baev, V.M.; Latz, T.; Toschek, P.E. Laser Intracavity Absorption Spectroscopy. *Appl. Phys. B* **1999**, *69*, 171. [CrossRef]
21. Durand, M.; Morville, J.; Romanini, D. Shot-noise-limited measurement of sub–parts-per-trillion birefringence phase shift in a high-finesse cavity. *Phys. Rev. A* **2010**, *82*, 031803. [CrossRef]
22. Flambaum, V.V.; Khriplovich, I.B. P-odd nuclear forces as a source of parity nonconservation in atoms. *Sov. Phys. JETP* **1980**, *52*, 835.
23. Flambaum, V.V.; Khriplovich, I.B.; Sushkov, O.P. Nuclear anapole moments. *Phys. Lett. B* **1984**, *146*, 367. [CrossRef]
24. Novikov, V.N.; Sushkov, O.P.; Flambaum, V.V.; Khriplovich, I.B. Possibility of studying the structure of weak neutral currents in optical transitions in heavy atoms. *Sov. Phys. JETP* **1977**, *46*, 420.
25. Flambaum, V.V.; Khriplovich, I.B. On the enhancement of parity nonconserving effects in diatomic molecules. *Phys. Lett. A* **1985**, *110*, 121. [CrossRef]
26. Zel'dovich, I.B. Electromagnetic Interaction with Parity Violation. *Sov. Phys. JETP* **1957**, *6*, 1184.
27. Landau, L.D.; Lifshitz, E.M. *Quantum Mechanics. Nonrelativistic Theory*; Pergamon: Oxford, UK, 1977.
28. Brown, J.M.; Carrington, A. *Rotational Spectroscopy of Diatomic Molecules*; Cambridge University Press: Cambridge, UK, 2003.
29. Bast, R.; Saue, T.; Visscher, L.; Jensen, H.J.; Bakken, V.; Dyall, K.G. DIRAC, a Relativistic ab Initio Electronic Structure Program, Release DIRAC15. 2015. Available online: http://www.diracprogram.org (accessed on 1 September 2019).
30. Kallay, M.M. MRCC, a quantum chemical program suite written by M. Kállay, Z. Rolik, I. Ladjánszki, L. Szegedy, B. Ladóczki, J. Csontos, and B. Kornis. Also see Rolik, Z. and Kàllay, M. A general-order local coupled-cluster method based on the cluster-in-molecule approach. *J. Chem. Phys.* **2011**, *135*, 104111. Available online: www.mrcc.hu (accessed on 1 September 2019).
31. Kallay, M.; Gauss, J. Approximate treatment of higher excitations in coupled-cluster theory. *J. Chem. Phys.* **2005**, *123*, 214105. [CrossRef]
32. Aquilante, F.; Vico, L.D.; Ferré, N.; Ghigo, G.; Malmqvist, P.-Å.; Neogrády, P.; Pedersen, T.B.; Pitonak, M.; Reiher, M.; Roos, B.O.; et al. MOLCAS 7: The next generation. *J. Comput. Chem.* **2010**, *31*, 224. [CrossRef]
33. Huber, K.P.; Herzberg, G. *Constants of Diatomic Molecules*; Van Nostrand-Reinhold: New York, NY, USA, 1979.
34. Sobel'man, I.I. *Atomic Spectra and Radiative Transitions*; Springer: Berlin/Heidelberg, Germany, 1980.
35. Kimball, D.F. Parity-nonconserving optical rotation on the $6s6p^3P_0 \rightarrow 6s6p^1P_1$ transition in atomic ytterbium. *Phys. Rev. A* **2001**, *63*, 052113. [CrossRef]